Nuclear matrix elements of neutrinoless double beta decay in MR-CDFT

Chenrong Ding

School of Physics and Astronomy, Sun Yat-Sen University

Collaborators: G. Li, J. Meng, P. Ring, J. M. Yao, X. Zhang

Nuclear Matrix Element Workshop (2023)

Osaka, Dec. 21-22, 2023

Introduction of Neutrinoless double beta decay

➢ What is $0\nu\beta\beta$?

$$X_Z^A \rightarrow Y_{Z+2}^A + e^- + e^-$$

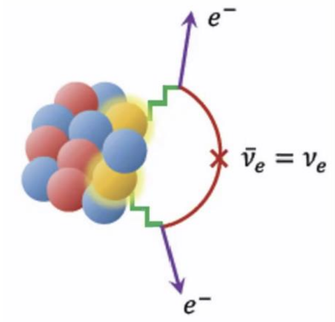

- Two neutrons decay into two protons, only two electrons emit
- Lepton number violation ($LNV = 2$) weak-interaction process

➢ Why is $0\nu\beta\beta$?

- Understand the nature of neutrinos
  - Absolute masses?
  - Majorana particle?
  - Ordering of masses?
- Discover new physics beyond Standard Model
  - Ultraviolet resonances?
  - A complete fundamental particle model?

Experimental researches of $0\nu\beta\beta$ decay

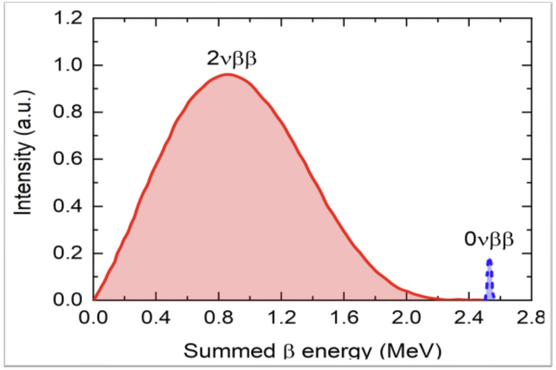

GERDA (^{76}Ge)

$T_{1/2}^{0\nu} > 1.8 \times 10^{26}$yrs

Phys.Rev.Lett.125(2020)252502

GUORE (^{130}Te)

$T_{1/2}^{0\nu} > 2.2 \times 10^{25}$yrs

Nature 604(2022)53

CUPID-0 (^{82}Se)

$T_{1/2}^{0\nu} > 2.4 \times 10^{24}$yrs

Phys.Rev.Lett.120(2018)232502

MAJORANA (^{76}Ge)

$T_{1/2}^{0\nu} > 8.3 \times 10^{25}$yrs

Phys.Rev.Lett.130(2023)062501

CUPID (^{100}Mo)

$T_{1/2}^{0\nu} > 1.5 \times 10^{24}$yrs

Phys.Rev.Lett.126(2021)181802

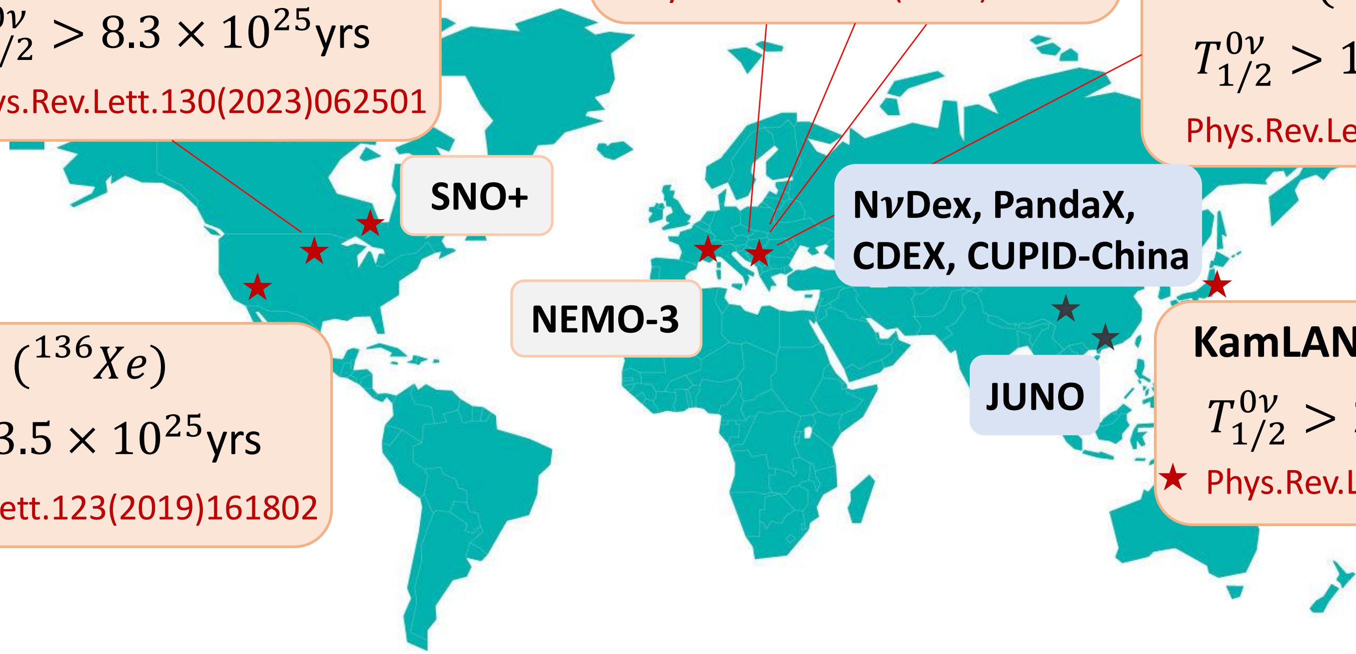

EXO-200 (^{136}Xe)

$T_{1/2}^{0\nu} > 3.5 \times 10^{25}$yrs

Phys.Rev.Lett.123(2019)161802

KamLAND-Zen (^{136}Xe)

$T_{1/2}^{0\nu} > 2.3 \times 10^{26}$yrs

★ Phys.Rev.Lett.130(2023)051801

Nuclear matrix element of $0\nu\beta\beta$ decay

- **Effective mass of neutrinos**

$$|\langle m_{\beta\beta}\rangle| = \left|\sum_{j=1}^{3} U_{ej}^2 m_j\right| = \left[\frac{m_e^2}{g_A^4 G_{0\nu} T_{1/2}^{0\nu} |M^{0\nu}|^2}\right]^{1/2}$$

$$M^{0\nu} = \langle \Psi_F | \hat{O}^{0\nu} | \Psi_I \rangle$$

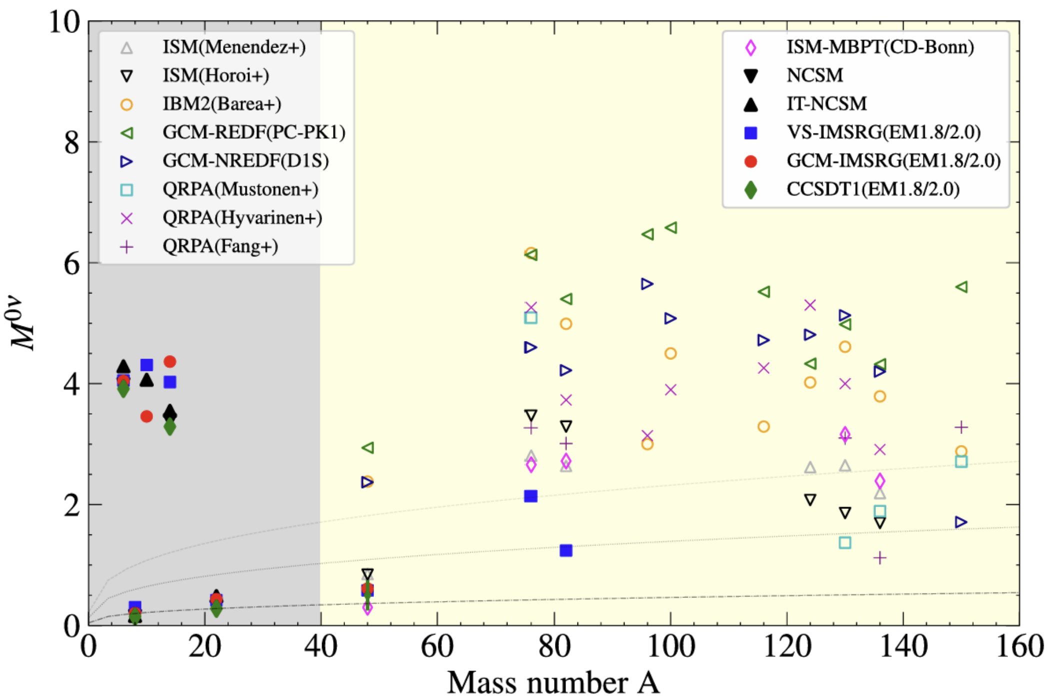

J. M. Yao et al., PPNP 126(2022)103965

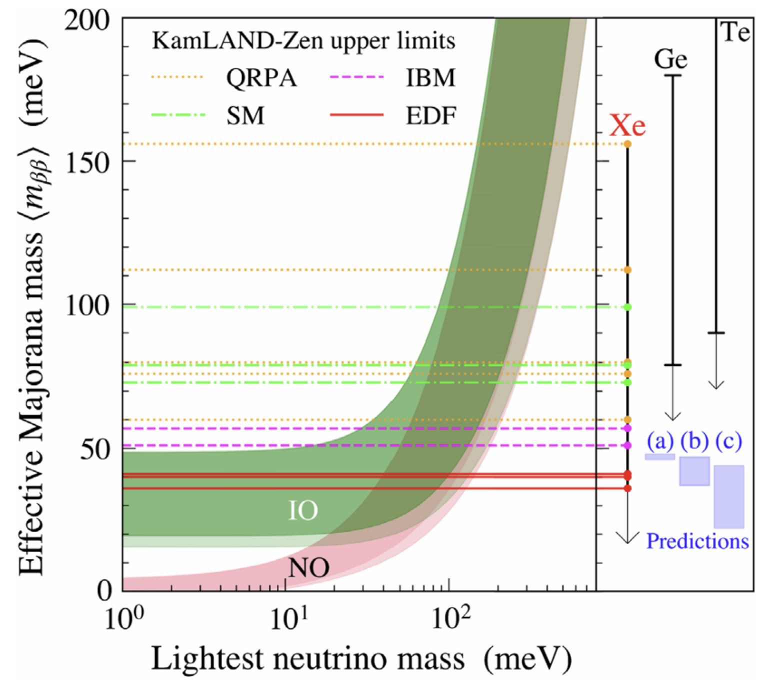

Phys.Rev.Lett.130(2023)051801

The RMF+BCS theory

- The point-coupling Lagrangian density

$$\begin{aligned}\mathcal{L}_{point} = {} & \bar{\varphi}(i\gamma_\mu\partial^\mu - m)\varphi - e\bar{\varphi}\gamma^\mu\frac{1-\tau_3}{2}\varphi A_\mu - \frac{1}{4}F^{\mu\nu}F_{\mu\nu} \\ & - \frac{1}{2}\alpha_S(\bar{\varphi}\varphi)(\bar{\varphi}\varphi) - \frac{1}{2}\alpha_V(\bar{\varphi}\gamma_\mu\varphi)(\bar{\varphi}\gamma^\mu\varphi) \\ & - \frac{1}{2}\alpha_{TV}(\bar{\varphi}\vec{\tau}\gamma_\mu\varphi)(\bar{\varphi}\vec{\tau}\gamma^\mu\varphi) - \frac{1}{2}\delta_S\partial_\nu(\bar{\varphi}\varphi)\partial^\nu(\bar{\varphi}\varphi) \\ & - \frac{1}{2}\delta_V\partial_\nu(\bar{\varphi}\gamma_\mu\varphi)\partial^\nu(\bar{\varphi}\gamma^\mu\varphi) - \frac{1}{2}\delta_{TV}\partial_\nu(\bar{\varphi}\vec{\tau}\gamma_\mu\varphi)\partial^\nu(\bar{\varphi}\vec{\tau}\gamma^\mu\varphi) \\ & - \frac{1}{3}\beta_S(\bar{\varphi}\varphi)^3 - \frac{1}{4}\gamma_S(\bar{\varphi}\varphi)^4 - \frac{1}{4}\gamma_V[(\bar{\varphi}\gamma_\mu\varphi)(\bar{\varphi}\gamma^\mu\varphi)]^2.\end{aligned}$$

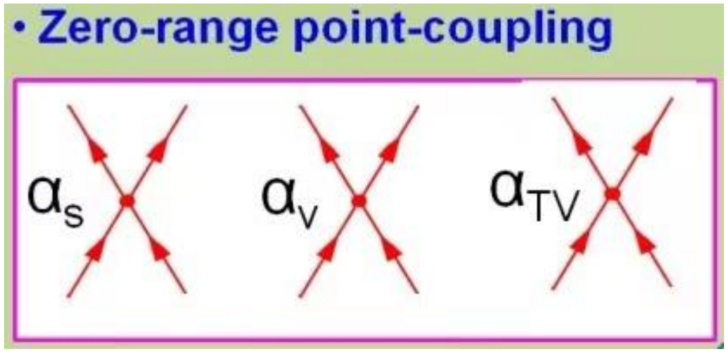

- Relativistic energy density functional

$$E = \langle\Phi_0|\hat{H}_0|\Phi_0\rangle$$

Here $|\Phi_0\rangle = \prod_{i=1}^{A}\hat{a}_i^\dagger|0\rangle$ is Slater determinant

- Single particle Dirac equation

$$[\boldsymbol{\alpha}\cdot(\boldsymbol{p}-\boldsymbol{V}) + V^0 + \beta(m+S)]\varphi_k = \epsilon_k\varphi_k$$

Here ϵ_k is single particle energy

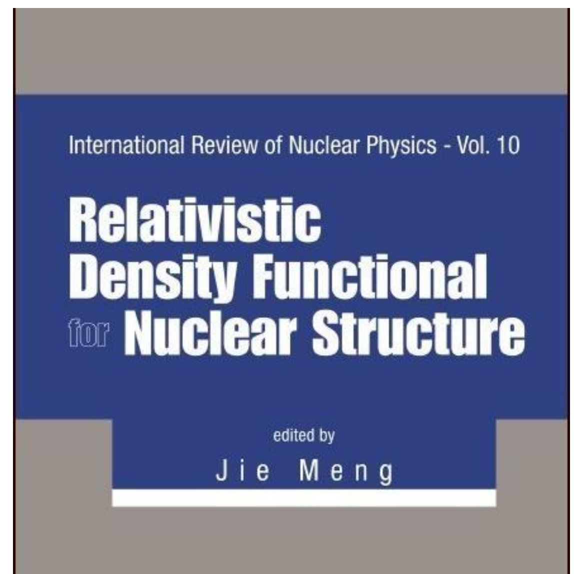

The RMF+BCS theory

- The mean-field wave function $|\Phi(\boldsymbol{q})\rangle$ are generated from the relativistic mean-field + Bardeen-Cooper-Schrieffer (RMF+BCS) theory with constraint on the mass quadrupole moment

$$\langle\Phi|\hat{H}|\Phi\rangle = \left\langle\Phi\left|\hat{H}_0 - \sum_{\tau=n,p}\lambda_\tau\hat{N}\right|\Phi\right\rangle - \frac{1}{2}\lambda_Q\left(\langle\Phi|\hat{Q}_{20}|\Phi\rangle - q_{20}\right)^2$$

and $|\Phi\rangle$ is the BCS state $|\Phi\rangle = \prod_{k>0}(u_k + v_k c_k^\dagger c_{\bar{k}}^\dagger)|0\rangle$

$$\left\langle\Phi\left|\hat{H}_0 - \sum_{\tau=n,p}\lambda_\tau\hat{N}\right|\Phi\right\rangle$$

$$= \sum_{k>0}\left[\left(2\epsilon_k - \sum_{\tau=n,p}2\lambda_\tau\right)v_k^2 - \int d\boldsymbol{r}\sum_{\tau=n,p}V_\tau\sum_{k'>0}f_k f_{k'}u_k v_k u_{k'}v_{k'}|\varphi_k(\boldsymbol{r})|^2|\varphi_{k'}(\boldsymbol{r})|^2\right]$$

Here V_τ is the pairing strengths. Solving the BCS equation

$$2(\epsilon_k - \lambda_\tau)v_k u_k + (f_k\Delta_k)\left(v_k^2 - u_k^2\right) = 0.$$

The BCS wave function is obtained.

The RMF+BCS theory

- The mean-field wave function $|\Phi(\boldsymbol{q})\rangle$ are generated from the relativistic mean-field + Bardeen-Cooper-Schrieffer (RMF+BCS) theory with constraint on the mass quadrupole moment

$$\langle\Phi|\hat{H}|\Phi\rangle = \left\langle\Phi\left|\hat{H}_0 - \sum_{\tau=n,p}\lambda_\tau\hat{N}\right|\Phi\right\rangle - \frac{1}{2}\lambda_Q\left(\langle\Phi|\hat{Q}_{20}|\Phi\rangle - q_{20}\right)^2$$

The second term generates mean-field states with different quadrupole deformations q_{20}

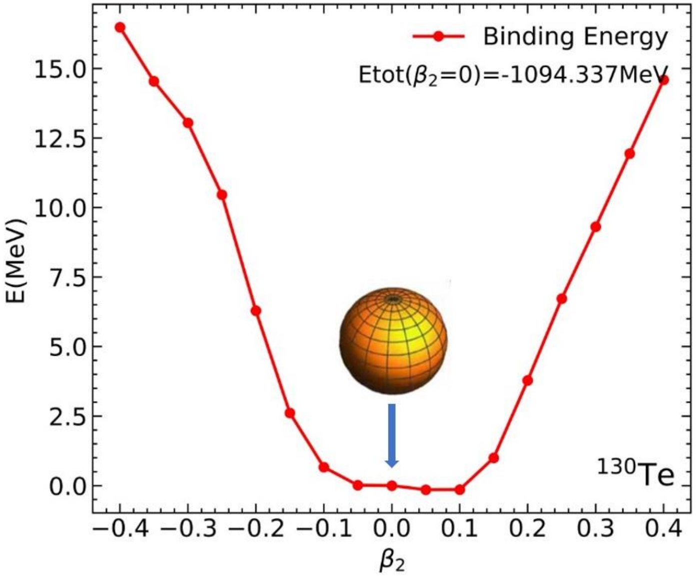

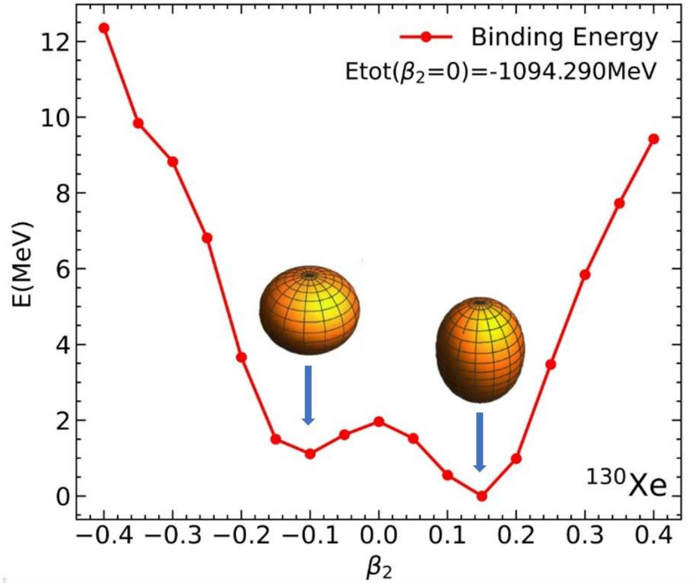

Generator coordinate method

- The angular momentum projected and particle number projected basis function is constructed as

$$|JMNZ,\boldsymbol{q}\rangle = \hat{P}^J_{M0}\,\hat{P}^N\,\hat{P}^Z|\Phi(\boldsymbol{q})\rangle$$

- The collective wave functions of nuclear low-lying states within the generator coordinate method (GCM)

$$|\Psi_\sigma^{JMNZ}\rangle = \sum_{\boldsymbol{q}} f_\sigma^J(\boldsymbol{q})\,|JMNZ,\boldsymbol{q}\rangle$$

- Through solving the Hill-Wheeler-Griffin (HWG) equation

P. Ring et al., *The nuclear many-body problem*, 1980.

$$\sum_{\boldsymbol{q}}\left[H^J_{00}(\boldsymbol{q},\boldsymbol{q}') - E^J_\sigma N^J_{00}(\boldsymbol{q},\boldsymbol{q}')\right] f^J_\sigma(\boldsymbol{q}') = 0 \quad \begin{cases} H^J_{00}(\boldsymbol{q},\boldsymbol{q}') = \langle\Phi(\boldsymbol{q})|\hat{H}\hat{P}^J_{00}\,\hat{P}^N\,\hat{P}^Z|\Phi(\boldsymbol{q}')\rangle \\ N^J_{00}(\boldsymbol{q},\boldsymbol{q}') = \langle\Phi(\boldsymbol{q})|\hat{P}^J_{00}\,\hat{P}^N\,\hat{P}^Z|\Phi(\boldsymbol{q}')\rangle \end{cases}$$

The weight functions $f_\sigma^J(\boldsymbol{q}')$ and the energies of low-lying states E_σ^J are obtained.

Multireference covariant density functional theory

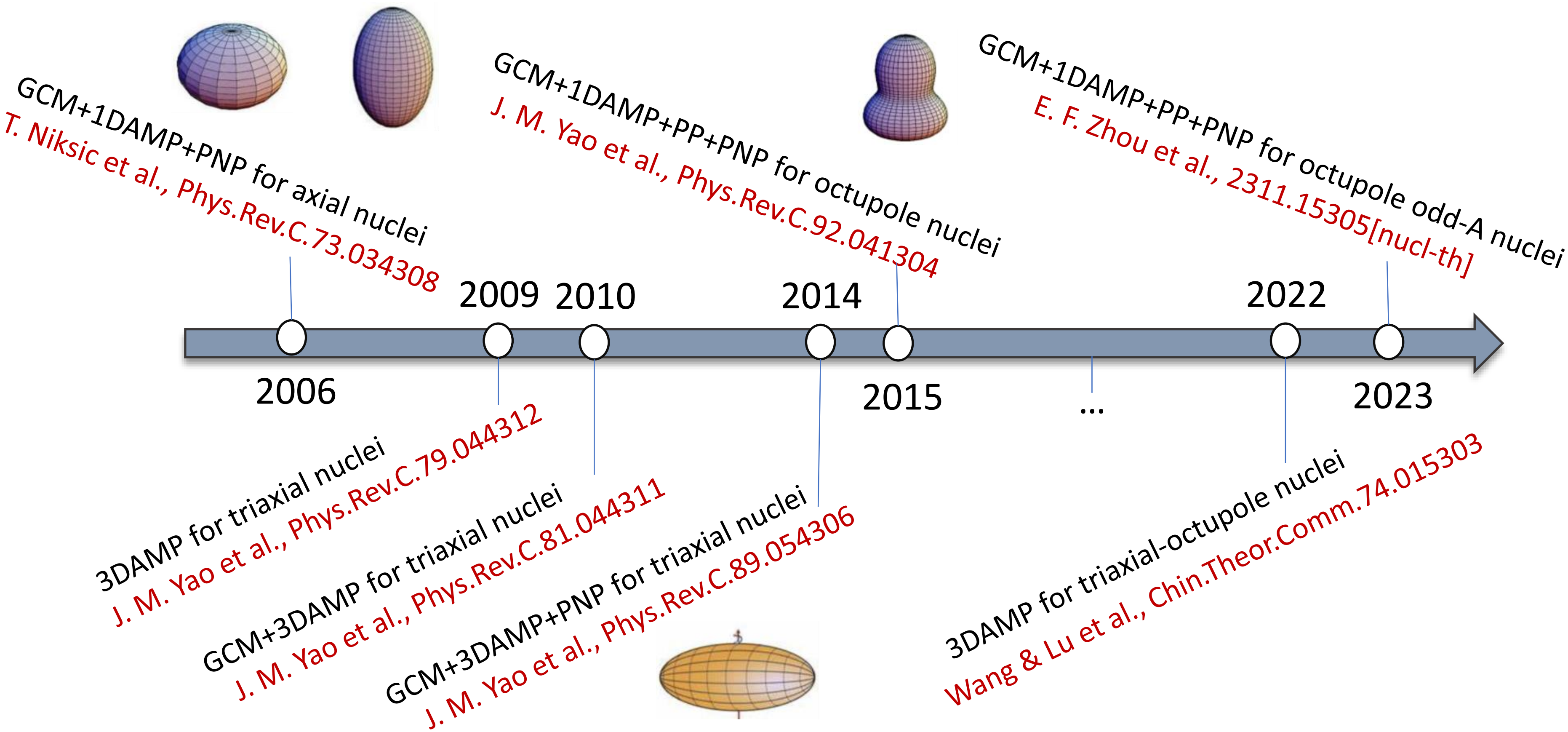

✓ **MR-CDFT has been applied to nuclei of all mass regions. The properties of nuclear low-lying states can be described well.**

The NME calculation of $0\nu\beta\beta$ decay

✓ **The nuclear collective wave function in MR-CDFT can be applied in the calculations of the NMEs of $0\nu\beta\beta$ decay.**

- The $0\nu\beta\beta$ decay NME for ^{150}Nd of standard mechanism (light neutrino exchange)

  L. S. Song et al., Phys.Rev.C.90(2014)054309

- Systematic study of the $0\nu\beta\beta$ decay NME for several candidate nuclei

  J. M. Yao et al., Phys.Rev.C.91(2015)024316

- The impact of Octupole correlations on the $0\nu\beta\beta$ decay NME for ^{150}Nd

  J. M. Yao et al., Phys.Rev.C.94(2016)014306

- The $0\nu\beta\beta$ decay NME by assuming the mechanism of exchanging heavy neutrinos

  L. S. Song et al., Phys.Rev.C.95(2017)024305

Nonstandard decay mechanisms

Nonstandard mechanisms in EFT framework

Framework of Effective field theory

Low-energy EFT (SM-EFT'):

After the electroweak symmetry breaking, match the LNV operators in SMEFT to the low energy scale.

V. Cirigliano et al., JHEP12(2018)097

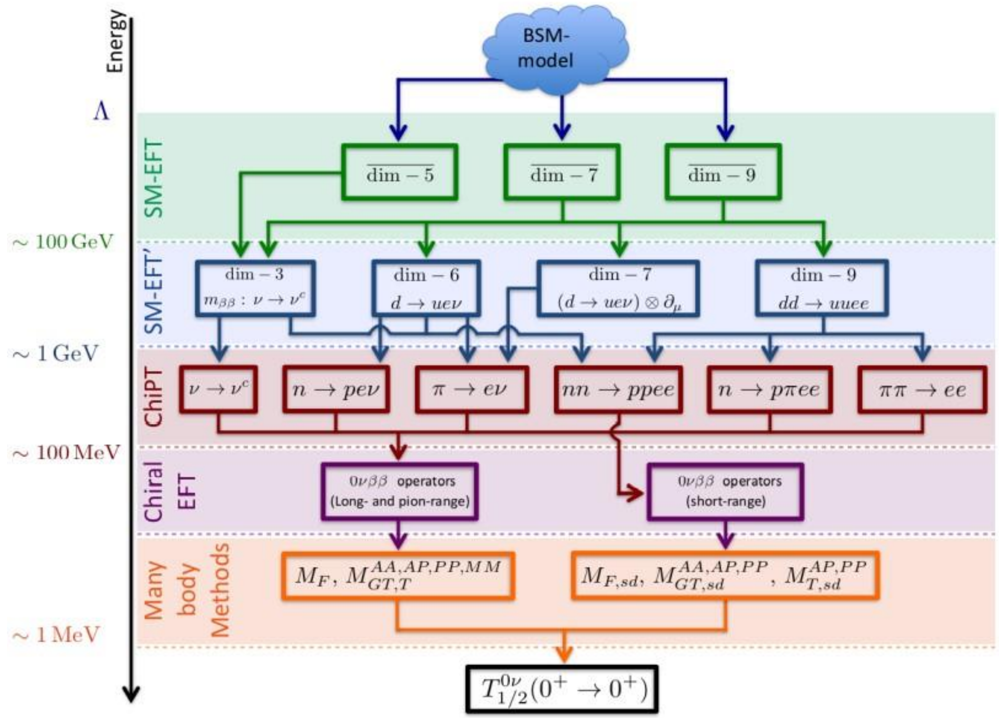

$$\mathcal{L}_{\Delta L=2} = -\frac{1}{2}(m_\nu)_{ij}\, \nu_{L,i}^T C \nu_{L,j} + \mathcal{L}_{\Delta L=2}^{(6)} + \mathcal{L}_{\Delta L=2}^{(7)} + \mathcal{L}_{\Delta L=2}^{(9)}$$

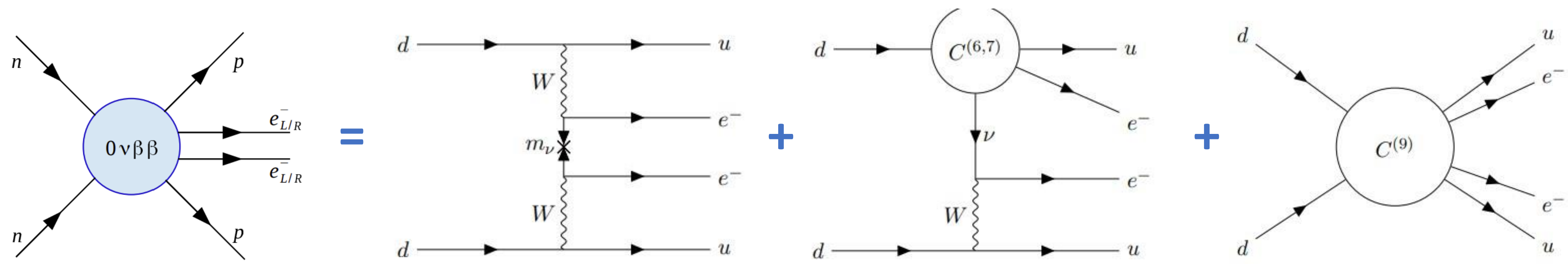

Low-energy effective field theory

V. Cirigliano et al., JHEP12(2018)097

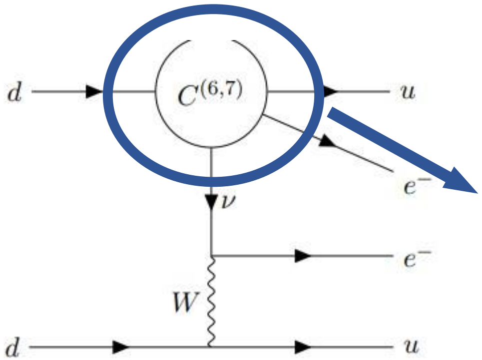

$$\mathcal{L}^{(6)}_{\Delta L=2} = \frac{2G_F}{\sqrt{2}}\Big(C^{(6)}_{\mathrm{VL},ij}\,\bar u_L\gamma^\mu d_L\,\bar e_{R,i}\,\gamma_\mu\,C\bar\nu^T_{L,j} + C^{(6)}_{\mathrm{VR},ij}\,\bar u_R\gamma^\mu d_R\,\bar e_{R,i}\,\gamma_\mu\,C\bar\nu^T_{L,j} + C^{(6)}_{\mathrm{SR},ij}\,\bar u_L d_R\,\bar e_{L,i}\,C\bar\nu^T_{L,j} + C^{(6)}_{\mathrm{SL},ij}\,\bar u_R d_L\,\bar e_{L,i}\,C\bar\nu^T_{L,j} + C^{(6)}_{\mathrm{T},ij}\,\bar u_L\sigma^{\mu\nu}d_R\,\bar e_{L,i}\sigma_{\mu\nu}\,C\bar\nu^T_{L,j}\Big)$$

$$\mathcal{L}^{(7)}_{\Delta L=2} = \frac{2G_F}{\sqrt{2}v}\Big(C^{(7)}_{\mathrm{VL},ij}\,\bar u_L\gamma^\mu d_L\,\bar e_{L,i}\,C\,i\overleftrightarrow{\partial}_\mu\bar\nu^T_{L,j} + C^{(7)}_{\mathrm{VR},ij}\,\bar u_R\gamma^\mu d_R\,\bar e_{L,i}\,C i\overleftrightarrow{\partial}_\mu\bar\nu^T_{L,j}\Big)$$

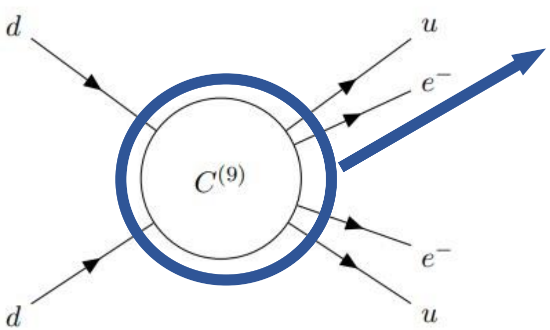

$$\mathcal{L}^{(9)}_{\Delta L=2} = \frac{1}{v^5}\sum_i\Big[\Big(C^{(9)}_{i\mathrm{R}}\,\bar e_R C\bar e^T_R + C^{(9)}_{i\mathrm{L}}\,\bar e_L C\bar e^T_L\Big)\,O_i + C^{(9)}_i\,\bar e\gamma_\mu\gamma_5 C\bar e^T\,O^\mu_i\Big],$$

$$O_1 = \bar q^\alpha_L\gamma_\mu\tau^+ q^\alpha_L\;\bar q^\beta_L\gamma^\mu\tau^+ q^\beta_L\,, \qquad O'_1 = \bar q^\alpha_R\gamma_\mu\tau^+ q^\alpha_R\;\bar q^\beta_R\gamma^\mu\tau^+ q^\beta_R\,,$$

$$O_2 = \bar q^\alpha_R\tau^+ q^\alpha_L\;\bar q^\beta_R\tau^+ q^\beta_L\,, \qquad O'_2 = \bar q^\alpha_L\tau^+ q^\alpha_R\;\bar q^\beta_L\tau^+ q^\beta_R\,,$$

$$O_3 = \bar q^\alpha_R\tau^+ q^\beta_L\;\bar q^\beta_R\tau^+ q^\alpha_L\,, \qquad O'_3 = \bar q^\alpha_L\tau^+ q^\beta_R\;\bar q^\beta_L\tau^+ q^\alpha_R\,,$$

$$O_4 = \bar q^\alpha_L\gamma_\mu\tau^+ q^\alpha_L\;\bar q^\beta_R\gamma^\mu\tau^+ q^\beta_R\,,$$

$$O_5 = \bar q^\alpha_L\gamma_\mu\tau^+ q^\beta_L\;\bar q^\beta_R\gamma^\mu\tau^+ q^\alpha_R\,,$$

- Dim-3 ($m_{\beta\beta}$)
- Dim-6 ($C^{(6)}_{SL}, C^{(6)}_{SR}, C^{(6)}_{VL}, C^{(6)}_{VR}, C^{(6)}_{T}$)
- Dim-7 ($C^{(7)}_{VL}, C^{(7)}_{VR}$)
- Dim-9 ($C^{(9)}_{iL}, C^{(9)}_{iR}, C^{(9)}_{i}$)

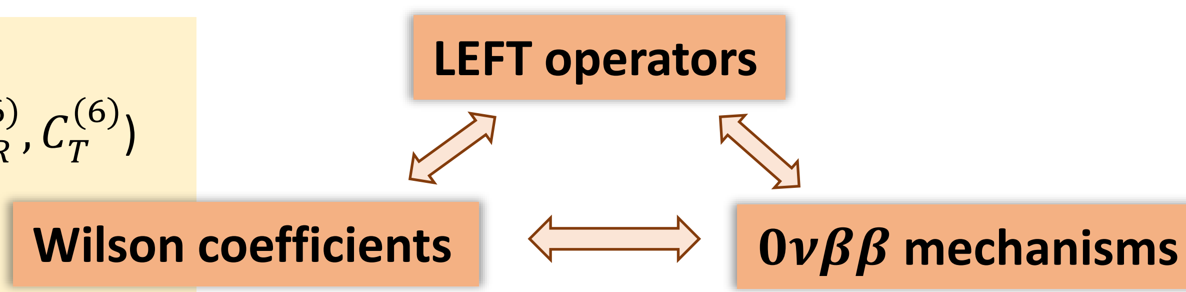

Half-life master formula in EFT framework

$$
\begin{aligned}
\left(T_{1/2}^{0\nu}\right)^{-1} = g_A^4 \Big\{ & G_{01}\left(|\mathcal{A}_\nu|^2 + |\mathcal{A}_R|^2\right) - 2\left(G_{01} - G_{04}\right)\mathrm{Re}\,\mathcal{A}_\nu^*\mathcal{A}_R + 4G_{02}\,|\mathcal{A}_E|^2 \\
& + 2G_{04}\left[\left|\mathcal{A}_{m_e}\right|^2 + \mathrm{Re}\left(\mathcal{A}_{m_e}^*\left(\mathcal{A}_\nu + \mathcal{A}_R\right)\right)\right] - 2G_{03}\,\mathrm{Re}\left[\left(\mathcal{A}_\nu + \mathcal{A}_R\right)\mathcal{A}_E^* + 2\mathcal{A}_{m_e}\mathcal{A}_E^*\right] \\
& + G_{09}\,|\mathcal{A}_M|^2 + G_{06}\,\mathrm{Re}\left[\left(\mathcal{A}_\nu - \mathcal{A}_R\right)\mathcal{A}_M^*\right]\Big\}
\end{aligned}
$$

V. Cirigliano et al., JHEP12(2018)097

The sub-amplitudes $\mathcal{A}_i$ contain various **WCs**, **low-energy constants(LECs)**, and **nuclear matrix elements(NMEs)**.

WCs, LECs: Unknown, power counting estimates.

NMEs ↓

Nuclear physics input

9 long-range NMEs: $M_F^{VV}, M_{GT}^{AA}, M_{GT}^{AP}, M_{GT}^{PP}, M_{GT}^{MM}, M_T^{AA}, M_T^{AP}, M_T^{PP}, M_T^{MM}$

6 short-range NMEs: $M_{F,sd}^{VV}, M_{GT,sd}^{AA}, M_{GT,sd}^{AP}, M_{GT,sd}^{PP}, M_{T,sd}^{AA}, M_{T,sd}^{AP}$

In our work, we performed separate calculations of NMEs for the exchange of light Majorana neutrinos and heavy neutrinos based on **MR-CDFT method**.

We decompose them into the 15 components, as the nuclear physics inputs, and conduct analyses on various decay mechanisms using the Master formula.

Results of NMEs and comparisons

The decomposed NMEs calculated by MR-CDFT method

CRD, et al., in preparation

NME	M_F	M_{GT}^{AA}	M_{GT}^{AP}	M_{GT}^{PP}	M_{GT}^{MM}	M_T^{AA}	M_T^{AP}	M_T^{PP}	M_T^{MM}	$M_{F,sd}$	$M_{GT,sd}^{AA}$	$M_{GT,sd}^{AP}$	$M_{GT,sd}^{PP}$	$M_{T,sd}^{AP}$	$M_{T,sd}^{PP}$
^{76}Ge	-1.924	5.743	-1.462	0.423	0.326	-	0.020	0.174	0.012	-2.226	7.141	-3.120	1.090	0.143	-0.226
^{82}Se	-1.742	5.021	-1.320	0.386	0.298	-	-0.018	0.156	0.005	-2.049	6.549	-2.882	1.011	0.023	-0.196
^{100}Mo	-1.814	6.341	-1.591	0.461	0.359	-	0.039	0.162	0.012	-2.484	7.974	-3.513	1.239	0.084	-0.284
^{130}Te	-1.365	4.565	-1.206	0.352	0.275	-	0.062	0.121	0.017	-1.843	6.160	-2.728	0.966	0.271	-0.270
^{136}Xe	-1.184	4.003	-1.059	0.308	0.240	-	0.053	0.108	0.014	-1.607	5.390	-2.379	0.841	0.221	-0.227

Comparison of the decomposed NMEs in ^{136}Xe that calculated by SM⋆, QRPA†, IBM2‡ and MR-CDFT. ⋆ J. Menéndez et al., JPG45.014003(2017) † J. Hyvärinen et al., PRC 91.024613(2015) ‡ F. F. Deppisch et al., PRD102.095016(2020)

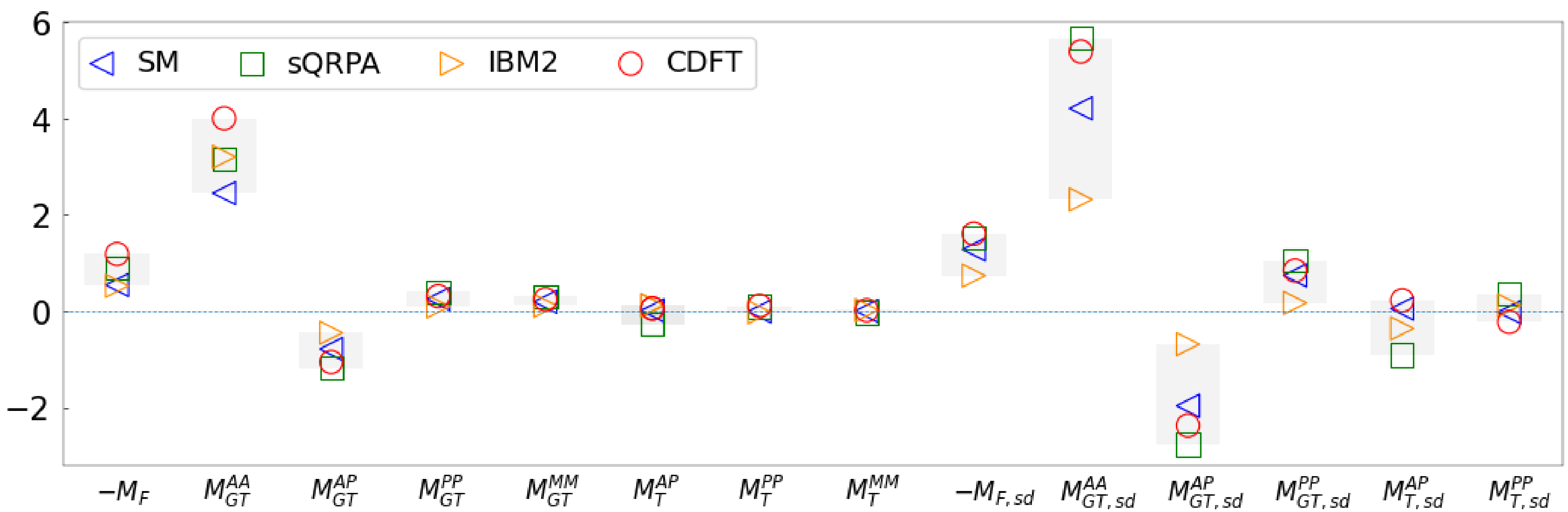

Constraints on Wilson coefficients

➢ Only consider the standard mechanism and single nonstandard mechanism

CRD, et al., in preparation

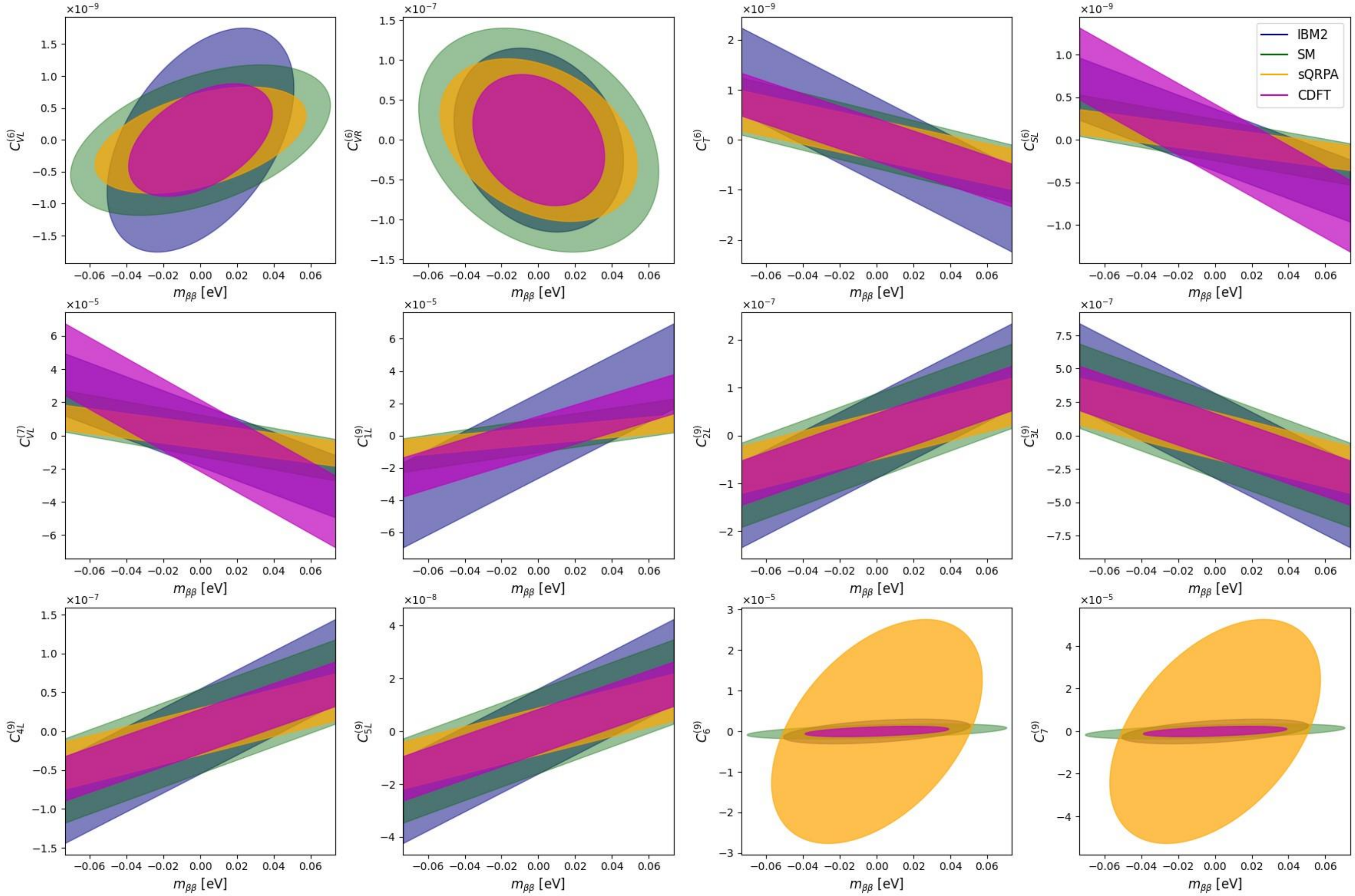

*The half-life $T_{1/2}^{0\nu} > 2.3 \times 10^{26}$yrs results from KamLAND-Zen Phys.Rev.Lett.130(2023)051801

Constraints on Wilson coefficients

➢ Only consider the standard mechanism and single nonstandard mechanism

CRD, et al., in preparation

- The related sub-amplitudes

$$\mathcal{A}_M = \frac{m_N}{m_e}\mathcal{M}_M^{(6)} + \frac{m_N^2}{m_e v}\mathcal{M}_M^{(9)}$$

- The NMEs combination

$$\mathcal{M}_M^{(9)} = \frac{m_\pi^2}{m_N^2}\Big[-\frac{2}{g_A^2}\left(g_6^{NN}C_V^{(9)} + g_7^{NN}\tilde{C}_V^{(9)}\right) M_{F,\,sd} + \frac{1}{2}\left(g_V^{\pi N}C_V^{(9)} + \tilde{g}_V^{\pi N}\tilde{C}_V^{(9)}\right)\left(M_{GT,\,sd}^{AP} + M_{T,\,sd}^{AP}\right)\Big]$$

$* \; C_V^{(9)} = C_6^{(9)}, \quad \tilde{C}_V^{(9)} = C_7^{(9)}$

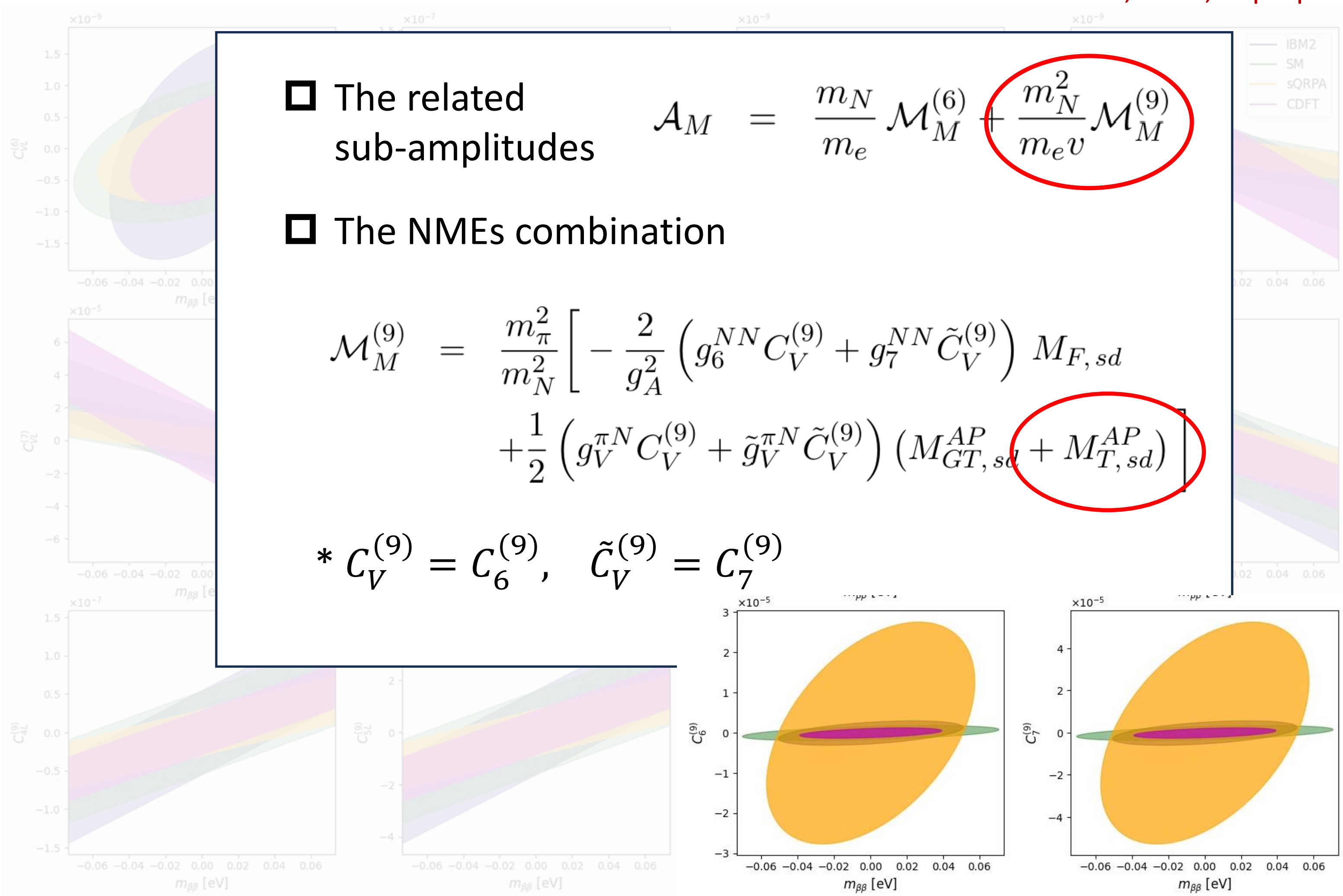

*The half-life $T_{1/2}^{0\nu} > 2.3 \times 10^{26}$yrs results from KamLAND-Zen Phys.Rev.Lett.130(2023)051801

Impact of isovector pairing correlations on NMEs

CRD, X. Zhang, J. M. Yao, P. Ring, J. Meng, Phys.Rev.C.108(2023)054304

Nuclear pairing correlations

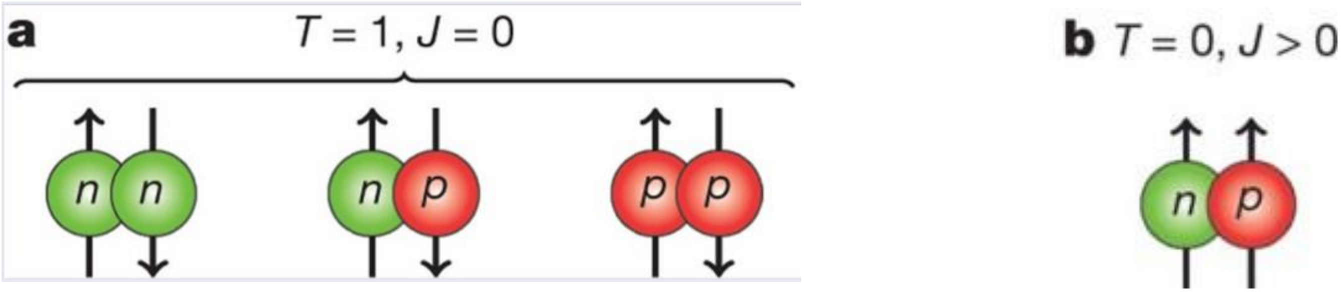

Isovector pairing

Isoscalar pairing

W.-L. Lv et al., PRC 108.L051304(2023)

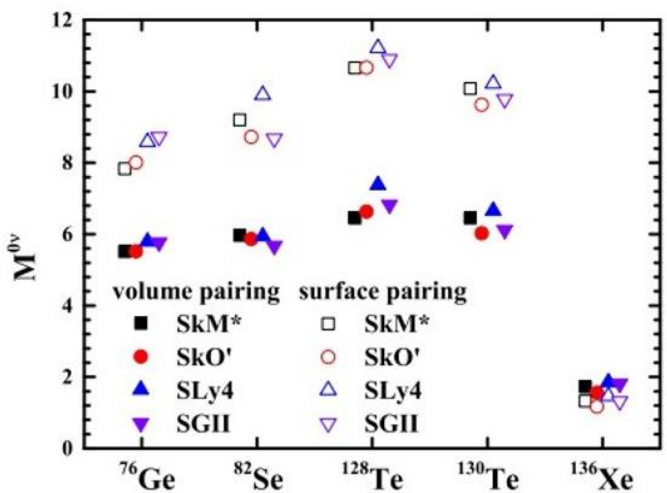

N. Hinohara & J. Engel,
PRC90, 031301(R) (2014)

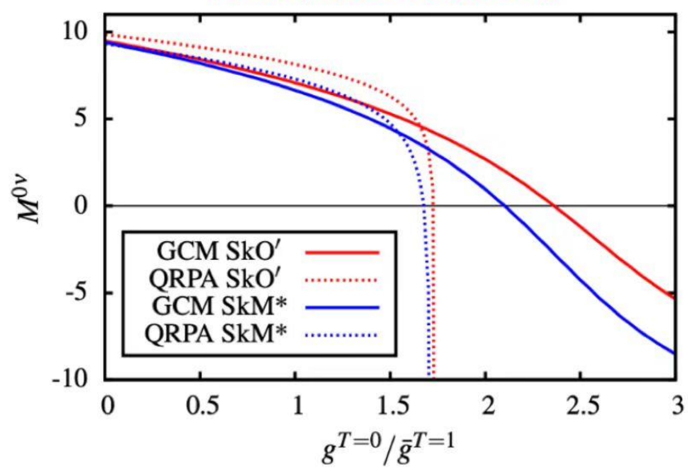

➢ **Properly addressing pairing correlation is important in NMEs calculation**

Readjust the isovector pairing strengths

➢ In MR-CDFT calculations, we find a linear correlation between the excitation energies of 2_1^+ and 4_1^+ states and the scaling factor χ, which multiplies the strength of isovector pairing field

$$V_\tau^{pp}(\boldsymbol{r_1}, \boldsymbol{r_2}) = \chi V_\tau^{pp} \delta(\boldsymbol{r_1} - \boldsymbol{r_2})$$

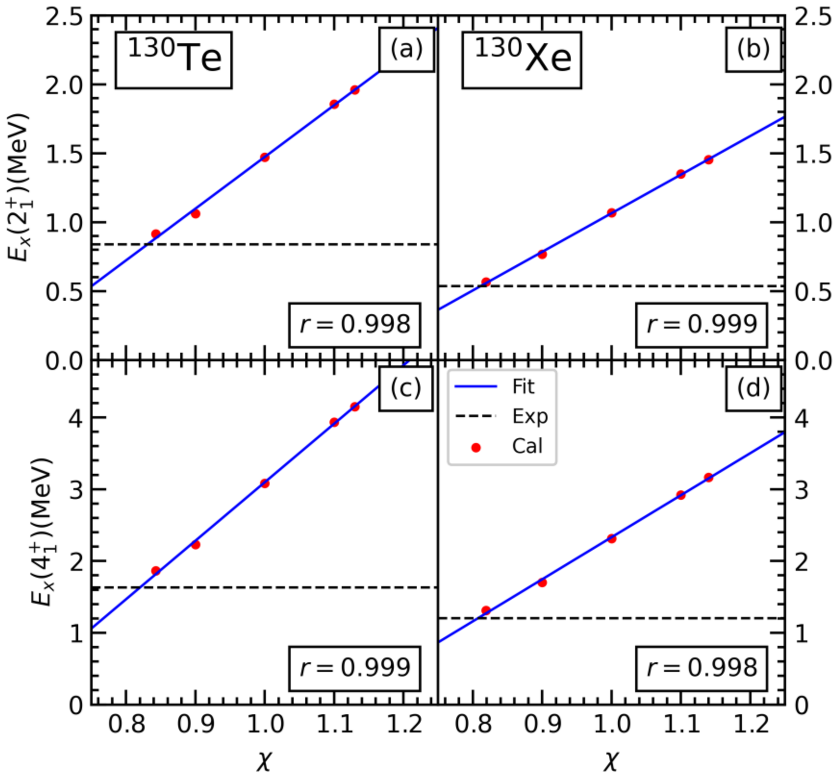

CRD, et al., Phys.Rev.C.108(2023)054304

Using the data of excitation energies, we readjust the isovector pairing strengths

^{76}Ge	^{76}Se	^{82}Se	^{82}Kr	^{100}Mo	^{100}Ru	^{130}Te	^{130}Xe	^{136}Xe	^{136}Ba
0.671	0.852	0.836	0.736	0.950	0.985	0.831	0.811	0.630	0.807

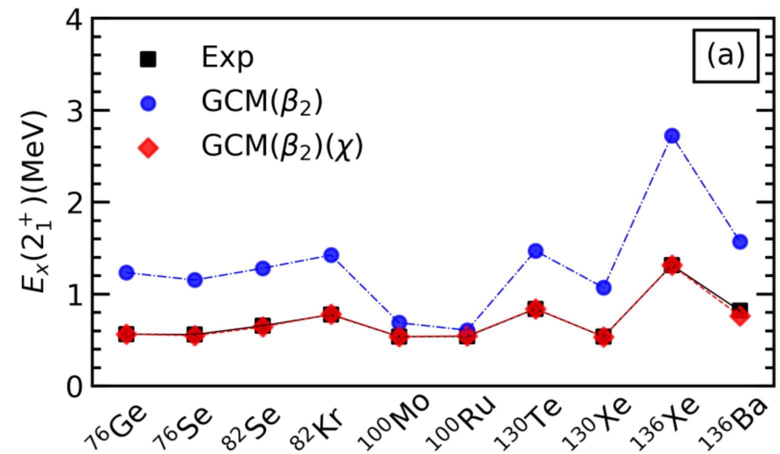

Isovector pairing fluctuation

- The mean-field wave function $|\Phi(\boldsymbol{q})\rangle$ are generated from the relativistic mean-field + Bardeen-Cooper-Schrieffer (RMF+BCS) theory with constraints on the mass quadrupole moment and isovector pairing amplitude

$$\langle\Phi|\hat{H}|\Phi\rangle = \left\langle\Phi\left|\hat{H}_0 - \sum_{\tau=n,p}\lambda_\tau\hat{N}\right|\Phi\right\rangle - \frac{1}{2}\lambda_Q\left(\langle\Phi|\hat{Q}_{20}|\Phi\rangle - q_{20}\right)^2 - \xi_p\left(\langle\Phi|\hat{P}_{T=1}|\Phi\rangle - P_1\right)$$

The last constraint term generates mean-field states with different isovector pairing amplitudes by introducing the operator

K. Sieja, et al., Eur.Phys,J.A 20(2004)413

$$\hat{P}_{T=1} = \frac{1}{2}\sum_{k>0}\left(c_k^\dagger c_{\bar{k}}^\dagger + c_k c_{\bar{k}}\right).$$

With the new constraint, the BCS equation

$$2(\epsilon_k - \lambda_\tau)v_k u_k + \left(f_k\Delta_k + \xi_p\right)\left(v_k^2 - u_k^2\right) = 0.$$

And the pairing gap $f_k\Delta_k$ is replaced by $f_k\Delta_k + \xi_p$. We can vary ξ_p and the pairing gap becomes a new generator coordinate.

N. L. Vaquero, et al., Phys.Rev.Lett.111(2013)142501

Isovector pairing fluctuation

Potential energy surfaces (mean-field level)

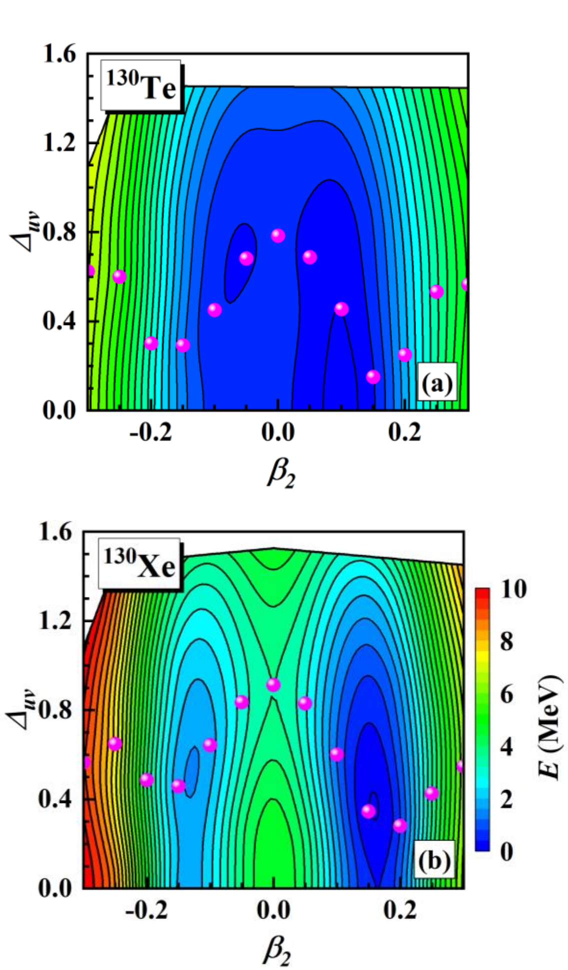

1DAMP

PNP

$J = 0$ potential energy surfaces

Collective ground state wave functions

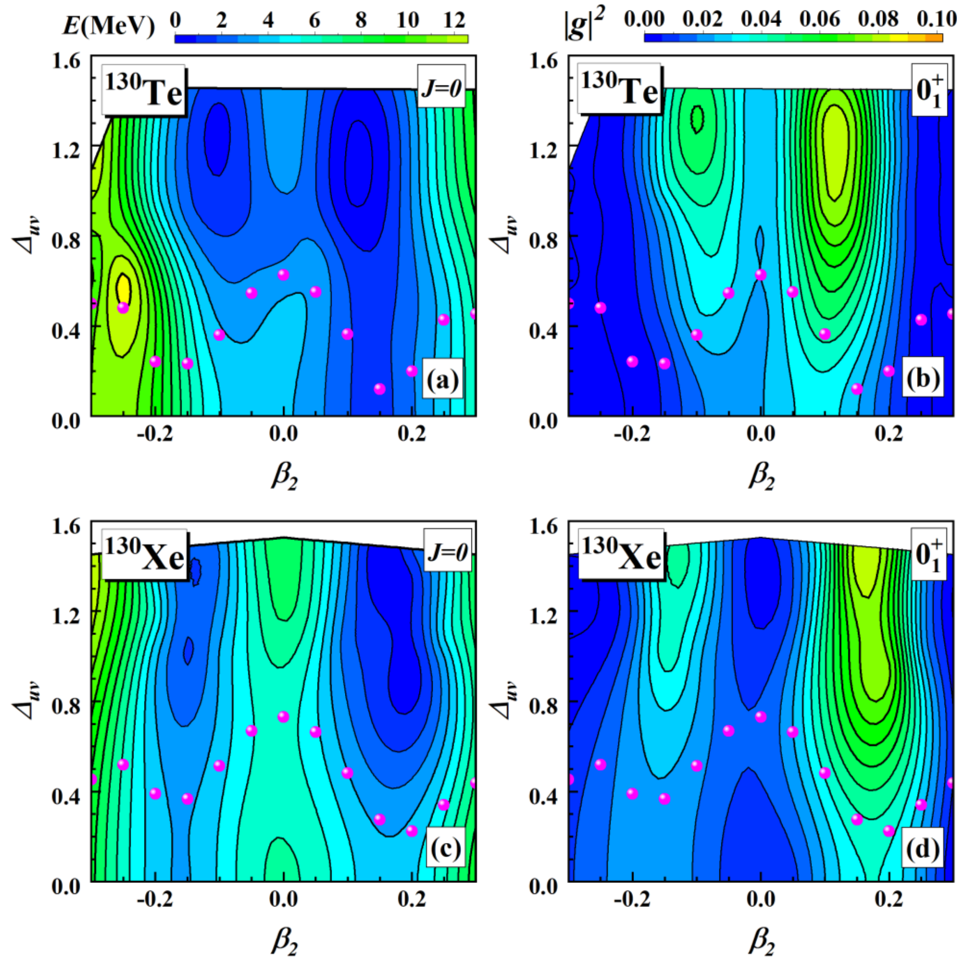

CRD, et al., Phys.Rev.C.108(2023)054304

Comparison of nuclear matrix elements

[21] L. S. Song, et al., Phys.Rev.C. 95(2017)024305

CRD, et al., Phys.Rev.C.108(2023)054304

	Isotopes	GCM(PC-PK1)(χ) This work	GCM(PC-PK1,β_2) [21]
	^{76}Ge	[2.37,6.34]	6.04
	^{82}Se	[2.46,5.68]	5.30
$M_\nu^{0\nu}$	^{100}Mo	[6.01,9.40]	6.48
	^{130}Te	[1.89,6.02]	4.89
	^{136}Xe	[2.27,5.06]	4.24
	^{76}Ge	[120.02,280.10]	209.1
	^{82}Se	[134.58,273.54]	189.3
$M_N^{0\nu}$	^{100}Mo	[289.17,444.59]	232.6
	^{130}Te	[113.06,315.79]	193.8
	^{136}Xe	[127.95,263.01]	166.3

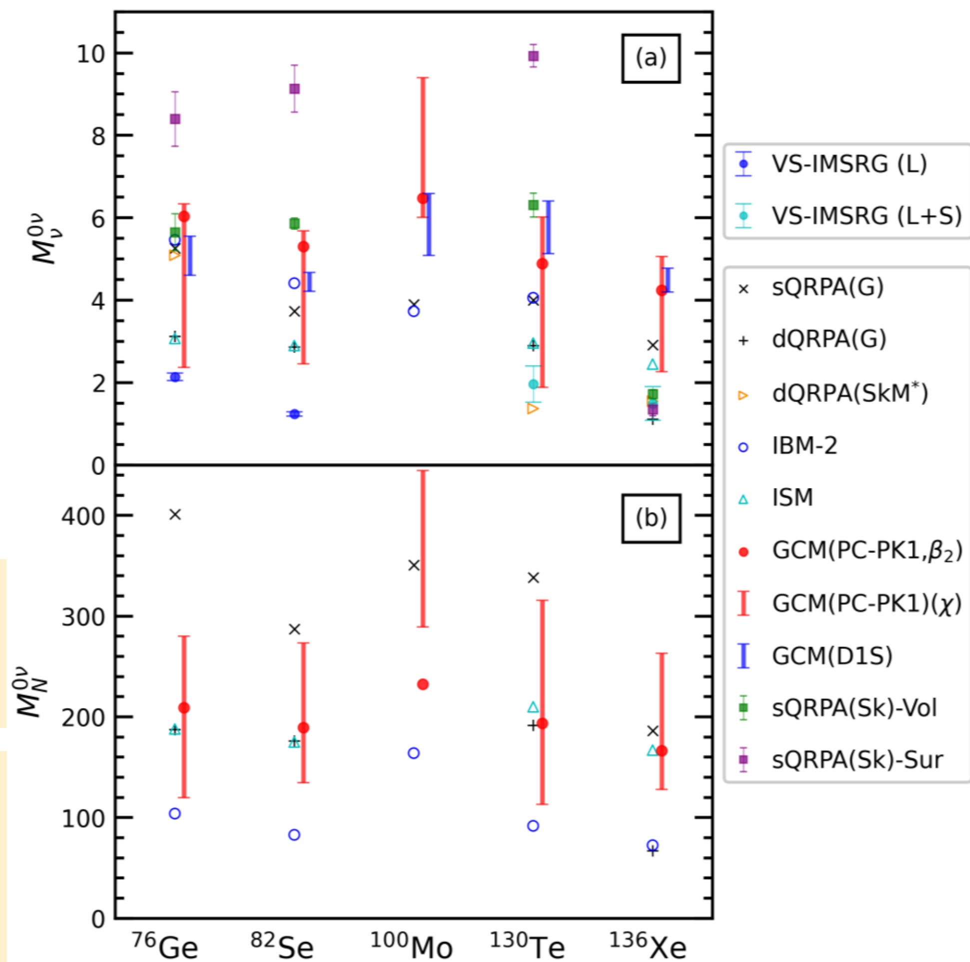

By readjusting pairing strengths, NMEs are reduced by approximately 12% − 62%.

By adding isovector pairing gap as an additional generator coordinate, NMEs increase by approximately 56% − 218%.

Summary and outlook

➢ Summary

1. The NMEs from different model calculations vary from each other, which leads to significant differences in the constraints on the Wilson coefficients.
2. In MR-CDFT, readjusting isovector pairing strengths reduces the NMEs by about $12\% - 62\%$.
3. In MR-CDFT, additionally including isovector pairing fluctuations enhances the NMEs by about $56\% - 218\%$.

➢ Outlook

1. Including the cranking states and the isoscalar pairing in MR-CDFT?
2. If the uncertainty in NMEs decreases, one can use the NMEs and experimental half-life results to constrain the Wilson coefficients, thus explore the complete particle model?

Thank you for your attention!